Supplementary file

Comparison of interdecadal precipitation variability over central North China and sub-Saharan Africa

Faustin Katchele OGOU[a,b], Qing YANG[a], Yawen DUAN[a] and Zhuguo MA[a,b]

[a]Chinese Academy of Sciences Key Laboratory of Regional Climate–Environment for Temperate East Asia, Institute of Atmospheric Physics, Chinese Academy of Sciences, Beijing 100029, China; [b]University of Chinese Academy of Sciences, Beijing 100049, China

This file includes:

Supplementary Text, Figures S1–S6, and Tables S1–S3

Study areas

Two regions are involved in the present study: CNC (35°–42.5°N, 110°–117.5°E) and SSA (2.75°–19.75°N, 17.75°W–51.75°E) (Figure S1).

CNC refers to a zone comprising Beijing city, Tianjin city, Hebei province, Shanxi province, and Inner Mongolia autonomous region, and is characterized by cold temperate, temperate, and warm temperate zones from north to south, and as a transitionary zone through semi-humid, semi-arid, and arid climate areas, in turn, from southeast to northwest, occasioning large climate differences (Guo et al. 2013). CNC is positioned in the central part of eastern China and at the northern limit of the East Asian summer monsoon region (Ren, Lu, and Xiao 2004).

For SSA, studies over a part or the entire area have examined the rainfall variability in various seasons and on different time scales (Bader 2003; Paeth et al. 2017). Additionally, the drought mechanisms have been examined over the region, owing to the dependency of the region's economy on agricultural activities (Wang et al. 2014). SSA's summer rainfall is organized through the West African monsoon, featuring large-amplitude, multi-decadal variability throughout the 20th century (Dong and Sutton 2015). The area is a semi-arid transition zone between the arid to hyper-arid Sahara and humid tropical Africa (Brooks 2004).

Correlation coefficient significance test

The significance of correlation coefficients after removing the auto-correlation by determining the effective degrees of freedom is tested. The effective degrees of freedom is applied to show the significance level as follows:

$$N^* = \frac{(N-1)(N-r_{\mathrm{xx}}(\mathrm{d}\tau)r_{\mathrm{yy}}(\mathrm{d}\tau))}{1+r_{\mathrm{xx}}(\mathrm{d}\tau)r_{\mathrm{yy}}(\mathrm{d}\tau)} \quad ,$$

where N, N^*, $r_{\mathrm{xx}}(\mathrm{d}\tau)$ and $r_{\mathrm{yy}}(\mathrm{d}\tau)$ represent the sample size, effective degrees of freedom and

autocorrelation of each SST modes and the NAO and precipitation time series, respectively, taking into account the low-frequency variability of the time series (Bretherton et al. 1999; Li et al. 2016). The Student's *t*-test is applied for the significance of the correlations using the formula

$$t = \sqrt{N-2} \times \frac{R}{\sqrt{1-R^2}}$$

where *R* represents the correlation coefficient between the two time series.

The covariance between the leading precipitation variability of SSA and CNC is assessed and presented in Table S2. Significant correlation coefficients between PCs of CNC and SSA are found.

References

Bader, J. 2003. "The Impact of Decadal-Scale Indian Ocean Sea Surface Temperature Anomalies on Sahelian Rainfall and the North Atlantic Oscillation." *Geophysical Research Letters* 30 (22): 1–4. doi:10.1029/2003GL018426.

Bretherton, C. S., M Widmann, V. P. Dymnikov, J. M. Wallace, and I. Blade. 1999. "Effective Number of Degrees of Freedom of a Spatial Field." *Journal of Climate* 12 (1969): 1990–2009. doi:Doi 10.1175/1520-0442(1999)012<1990:Tenosd>2.0.Co;2.

Brooks, N. 2004. "Drought in the African Sahel: Long Term Perspectives and Future Prospects." *Tyndall Centre for Climate Change Research*, no. October. http://citeseerx.ist.psu.edu/viewdoc/download?doi=10.1.1.151.8727&rep=rep1&type=pdf%5Cnpapers2://publication/uuid/81C009F8-5A32-4BA3-B927-FE1EA2608311.

Dong, B., and R. Sutton. 2015. "Dominant Role of Greenhouse-Gas Forcing in the Recovery of Sahel Rainfall." *Nature Climate Change* 5 (8). Nature Publishing Group: 757–60.

doi:10.1038/nclimate2664.

Gao, H., and S. Yang. 2009. “A Severe Drought Event in Northern China in Winter 2008-2009 and the Possible Influences of La Niña and Tibetan Plateau.” *Journal of Geophysical Research Atmospheres* 114 (24): 1–16. doi:10.1029/2009JD012430.

Guo, W.-L., S. Hong-Bo, M. Jing-Jin, Z. Ying-Juan, W. Ji, S. Wen-Jun, and Z. Zi-Yin. 2013. “Basic Features of Climate Change in North China during 1961–2010.” *Advances in Climate Change Research* 4 (2). Elsevier Masson SAS: 73–83. doi:10.3724/SP.J.1248.2013.073.

Li, L., R. W. Schmitt, C. C. Ummenhofer, and K. B. Karnauskas. 2016. “North Atlantic Salinity as a Predictor of Sahel Rainfall.” *Science Advances* 2 (5). http://advances.sciencemag.org/content/2/5/e1501588.abstract.

Paeth, H., A. Paxian, D. V. Sein, D. Jacob, H. J. Panitz, M. Warscher, A. H. Fink, et al. 2017. “Decadal and Multi-Year Predictability of the West African Monsoon and the Role of Dynamical Downscaling.” *Meteorologische Zeitschrift* 26 (4): 363–77. doi:10.1127/metz/2017/0811.

Ren, B. H., R. Y. Lu, and Z. N. Xiao. 2004. “A Possible Linkage in the Interdecadal Variability of Rainfall over North China and the Sahel.” *Advances in Atmospheric Sciences* 21 (5): 699–707. doi:10.1007/BF02916367.

Wang, Q., J. Wu, T. Lei, B. He, Z. Wu, M. Liu, X. Mo, et al. 2014. “Temporal-Spatial Characteristics of Severe Drought Events and Their Impact on Agriculture on a Global Scale.” *Quaternary International* 349. Elsevier Ltd: 10–21. doi:10.1016/j.quaint.2014.06.021.

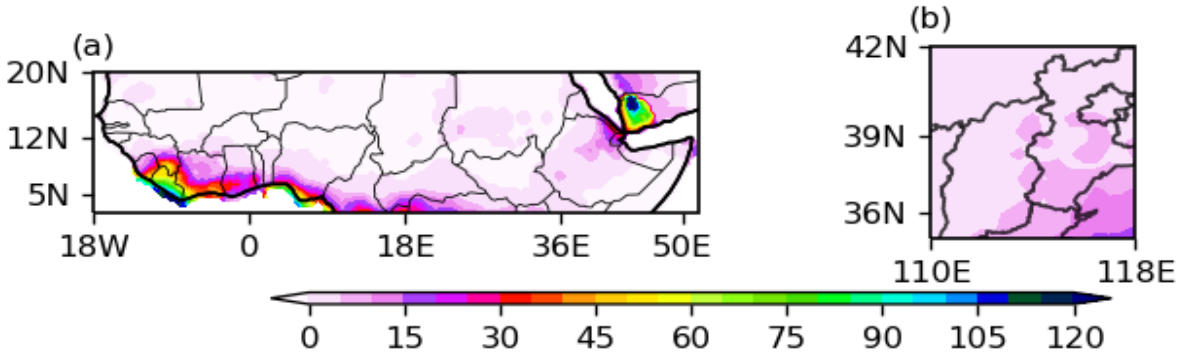

Figure S1. The distribution of climatic precipitation (average 1951−2010, units: mm/month) over (a) SSA and (b) CNC.

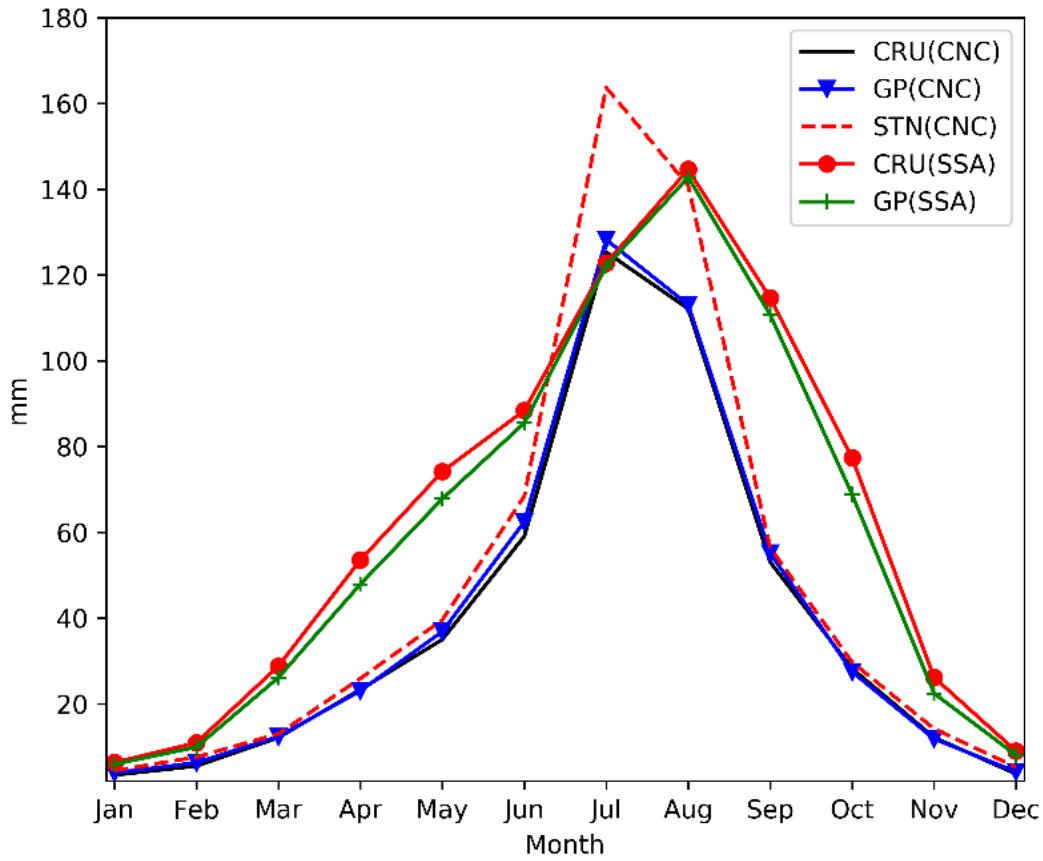

Figure S2. Annual cycle of precipitation in SSA and CNC using different datasets.

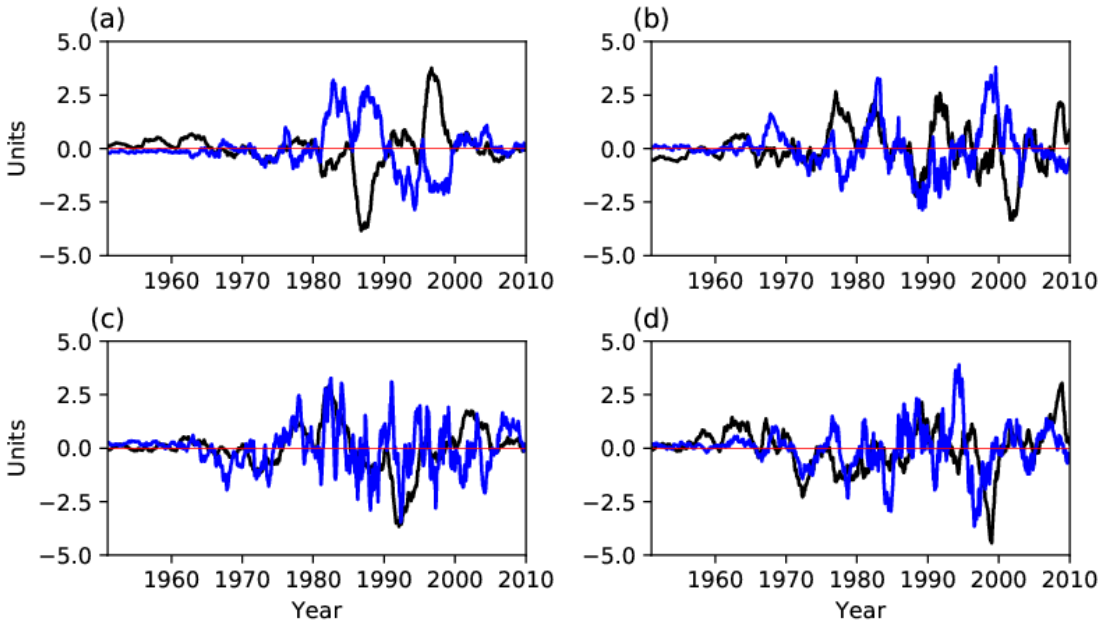

Figure S3. Time series of PCs of CNC (blue line) and SSA (black line). The red and dashed red lines indicate the references and extremes values, respectively. Panels (a) to (d) are the PC1s, PC2s, PC3s, and PC4s of the precipitation variability, respectively.

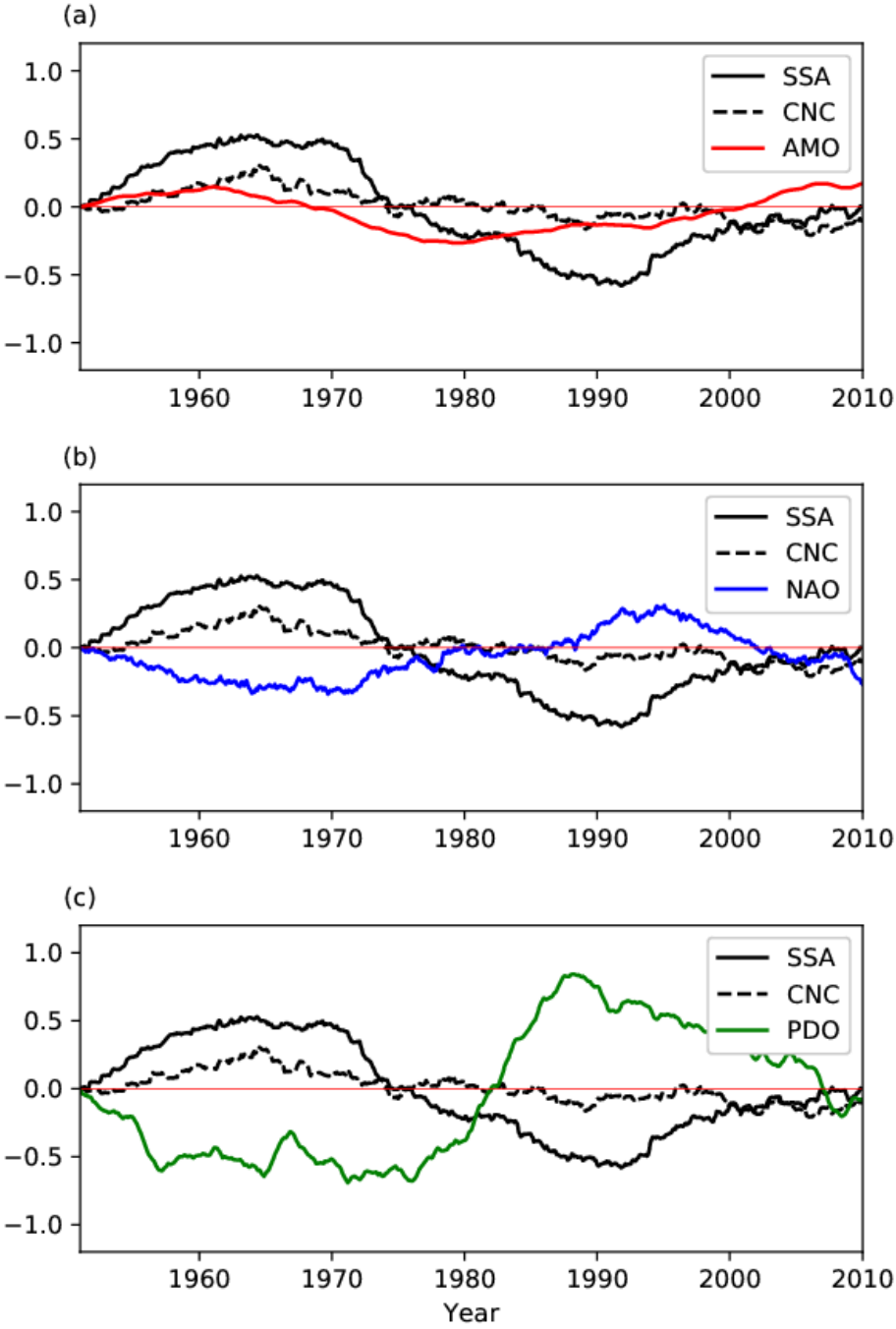

Figure S4. Time series of the decadal precipitation anomalies over SSA and CNC, as well as the (a) AMO, (b) NAO, and (c) PDO indices.

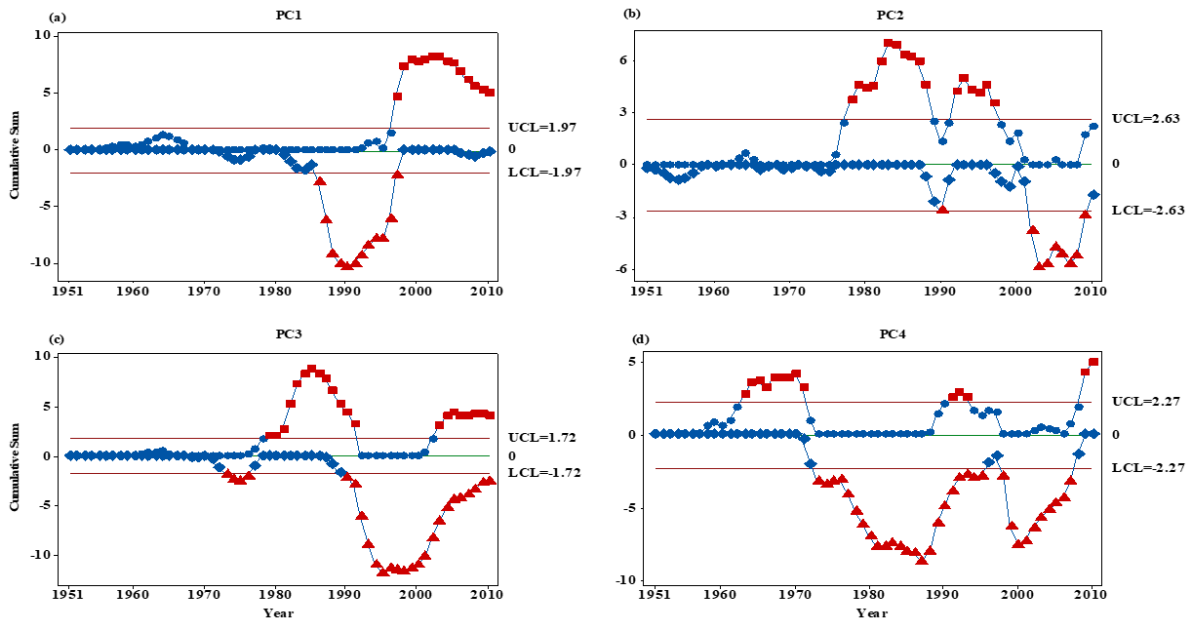

Figure S5. Shifts in PCs of SSA via cumulative sum chart. The deviation of the blue lines from the references and located between the limit lines (red) show the origins of the shifts observed. Significant shifts are shown as red points. Panels (a) to (d) correspond to PC1 to PC4, respectively.

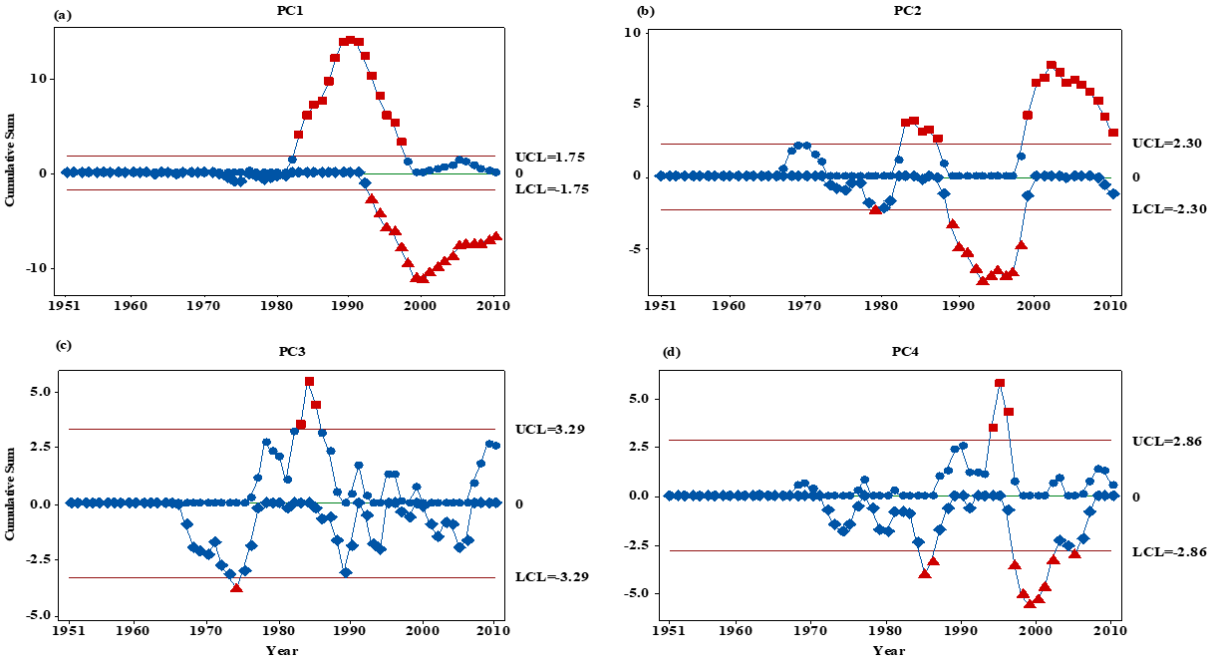

Figure S6. The same as Figure S5, but for CNC.

Table S1. Station data in CNC.

No	STN_ID	STN_NAME	Longitude (°E)	Latitude (°N)
1	CHM00054916	YANZHOU	116.850	35.567
2	CHM00054823	JINAN	117.050	36.600
3	CHM00054725	HUIMIN	117.533	37.500
4	CHM00054511	CHM00054511	116.283	39.933
5	HUIMIN, CH	ANYANG	114.400	36.050
6	CHM00053772	TAIYUAN	112.550	37.783
7	CHM00053463	HOHHOT	111.683	40.817

Table S2. Correlation coefficients between PCs of SSA and CNC. The values in bold indicate the correlation coefficient passing statistically significant test at the 0.05 level.

	PC1	PC2	PC3	PC4
Corr (CNC, SSA)	**−0.65**	−0.03	**0.34**	0.23

Table S3. Shift years identified in the decadal variability of precipitation. The first and second rows for each region (SSA and CNC) indicate positive (+) and negative (−) shifts, respectively.

		PC1	PC2	PC3	PC4
SSA	+	1997	1978, 1992	1979, 2003	1963, 1991, 2009
	–	1986	1990, 2002	1973, 1990	1973, 1998
CNC	+	1983	1983, 1999	1983	1994
	–	1993	1979, 1989	1974	1985, 1997, 2005